Applied Catalysis B: Environmental 224 (2018) 919–927

Contents lists available at ScienceDirect

Applied Catalysis B: Environmental

journal homepage: www.elsevier.com/locate/apcatb

# Methanation of $CO_2$ over alkali-promoted $Ru/TiO_2$ catalysts: I. Effect of alkali additives on catalytic activity and selectivity

Athanasia Petala[a], Paraskevi Panagiotopoulou[b,*]

[a] Department of Chemical Engineering, University of Patras, GR-26504 Patras, Greece
[b] School of Environmental Engineering, Technical University of Crete, GR-73100 Chania, Greece

ARTICLE INFO

*Keywords:*
$CO_2$ hydrogenation reaction
Methane
Ruthenium
Titanium dioxide
Alkali promotion

ABSTRACT

The effect of alkali promotion of $TiO_2$ on the $CO_2$ hydrogenation activity and selectivity has been investigated over 0.5%$Ru/TiO_2$ and 5%$Ru/TiO_2$ catalysts of different promoter type (Li, Na, K, Cs) and variable promoter loading (0.0–0.40 wt.%). The effect of alkali promotion was found to be more pronounced over catalysts of low Ru loading (or small Ru crystallites). In the case of 0.5%$Ru/TiO_2$ catalysts, both catalytic activity and methane selectivity are strongly enhanced with the addition of small amounts (0.2 wt.%) of alkalis following the order of $TiO_2$ (unpromoted) < Li ~ K < Cs < Na. The intrinsic reaction rate exhibits a volcano-type dependence on the sodium content. Optimal results were obtained for 0.5%$Ru/TiO_2$ catalyst containing 0.2 wt.% Na, the specific activity of which is about 3 times higher, compared to that of the unpromoted sample. In the case of 5%$Ru/TiO_2$ catalysts, alkali addition does not practically affect catalytic activity and selectivity. Turnover frequency of 0.5%Ru/0.2%Na-$TiO_2$ catalyst is higher than that measured over 5%$Ru/TiO_2$, indicating that small amounts of alkalis can replace part of precious metals, reducing the cost and increasing the efficiency of the $CO_2$ methanation process.

## 1. Introduction

Carbon dioxide ($CO_2$) elimination has been the subject of numerous studies due to the adverse environmental effects induced by $CO_2$ emissions in the atmosphere, such as global warming and subsequent major climate changes [1–5]. Reduction of $CO_2$ can be achieved using various methods, including storage, separation and utilization via its conversion to added value chemicals and fuels [1,2,6,7]. Among various processes, the interaction of $CO_2$ with sustainable hydrogen producing methane (Eq. (1)) can be considered as a promising method for $CO_2$ elimination. Methane produced can be used in chemical industry as synthetic substitute of natural gas and/or in power plants as energy carrier, which can be stored in the natural gas grid [1,3,4,6–9].

$$CO_2 + 4H_2 \leftrightarrow CH_4 + 2H_2O,\ \Delta H^o = -165\ kJ/mol \quad (1)$$

Concerning $CO_2$ methanation mechanism, two general schemes have been proposed depending on the metal-support combination employed. The first scheme includes $CO_2$ dissociation on the catalyst surface toward adsorbed CO and oxygen species, followed by interaction of the dissociated species with $H_2$ resulting in $CH_4$ formation [3,10–13]. The second scheme is most common over supported Ru catalysts and proceeds through intermediate formation of adsorbed carbonyl species via the reverse water-gas shift (RWGS) reaction (Eq. (2)) [7,14–20].

$$CO_2 + H_2 \leftrightarrow CO + H_2O\ \Delta H^o = 41.1\ kJ/mol \quad (2)$$

Part of this species interacts with adsorbed hydrogen atoms to form methane, following either CO dissociation and subsequent hydrogenation of surface carbon toward methane [10,11,20–22] or an associative pathway, which involves the formation of an oxygen-containing carbonyl species and, eventually, methane in the gas phase [11,15,23–25]. The remaining adsorbed carbonyl species is desorbed yielding CO in the gas phase in a manner which depends strongly on the catalyst and the experimental conditions (e.g. temperature, feed composition etc.) employed, determining selectivity toward $CH_4$ or CO [10,16].

Results of our previous studies clearly indicated that $CO_2$ methanation reaction over $Ru/TiO_2$ catalysts proceeds via the RWGS reaction through the associative CO hydrogenation pathway [15,23]. Consequently, it is important to develop $CO_2$ methanation catalysts with sufficiently high activity at relative low temperatures (< 400 °C), able to enhance the hydrogenation of intermediate CO, suppressing it's desorption in the gas phase.

Previous studies have shown that catalytic activity and selectivity for the $CO_2$ hydrogenation reaction depend strongly on the nature of

* Corresponding author.
*E-mail address:* ppanagiotopoulou@isc.tuc.gr (P. Panagiotopoulou).

https://doi.org/10.1016/j.apcatb.2017.11.048
Received 11 July 2017; Received in revised form 25 October 2017; Accepted 17 November 2017
Available online 20 November 2017

the dispersed metallic phase, metal crystallite size as well as the support employed [26,27]. Generally, supported Rh [1,3,6,28–30], Ru [18–20,30–34] and Ni [5,35–37] catalysts seem to present high activity and selectivity toward $CH_4$ at low temperatures, which can be enhanced with increasing metal loading and/or crystallite size [27,30]. Although the cost of Ni based catalysts is significantly lower than that of Ru and/or Rh based catalysts, Ni catalysts have been reported to be easily deactivated due to carbon deposition, sintering of Ni particles and/or formation of mobile nickel sub-carbonyls [38,39]. On the other hand, supported Ru catalysts have been reported to exhibit excellent stability over a wide range of operating conditions [20,40] and thus, they may are preferred for $CO_2$ methanation reaction.

Metal-support interactions can modify the catalytic properties of the metallic phase and therefore, the nature of the support plays a crucial role in the reaction pathway [27,41]. Among various supports investigated, $TiO_2$-supported catalysts have been found to exhibit enhanced $CO_2$ methanation activity and selectivity. The beneficial effect of $TiO_2$ support has been attributed either to electronic interactions between the support and the dispersed metal [17,20,41–43] or to interactions of $Ti^{3+}$ ions, located in the vicinity of metal adsorption sites, with CO adsorbed on metal [44,45]. These interactions have been proposed to facilitate the dissociation of C—O bond, thereby enhancing the $CO_2$ hydrogenation activity.

Efforts have been made to improve catalytic activity and selectivity of Ni, Rh and Ru catalysts via doping of $Al_2O_3$ [2,46], $TiO_2$ [41,43], $SiO_2$ [47,48] and $ZrO_2$ [49] supports with various additives, such as alkali (Na, K, Li, Cs) [46,47], alkaline earths (Ca, Ba, Sr, Mg) [43,46,48], lanthanides (La, Ce) [46] as well as transition metals (Ni, Co, Zr, W) [41,43,46]. It is of interest to note that, among the studies reported so far on the effect of alkali promotion, only a few, at least to our knowledge, reported improved catalytic activity for the $CO_2$ methanation reaction [47,50–54]. In particular, Li et al. [54] attributed the promoting ability of alkalis over $Ru/Al_2O_3$ catalysts to a synergetic effect, including modification of Ru electron density due to the electron-donating character of alkalis, the neutralization of residual chlorine ions of metal precursor and the facilitation of the removal of inactive carbon deposited on catalyst surface under reaction conditions. Duyar et al. [53] reported that K and Na can act as $CO_2$ adsorbents, resulting in enhancement of methanation capacities and thus, improving the performance of $5\%Ru/Al_2O_3$ catalysts. FTIR studies over K-promoted Ru(001) showed a dual function of potassium promoter, by favoring the dissociation of CO and directly participating in the formation of formate intermediate species [55]. An et al. [52] found that the presence of K over $Cu_xO/Cu(111)$ catalyst was able to accelerate $CO_2$ activation in a manner which depends strongly on both geometric and electronic effects. On the other hand, the modification of $Rh/Al_2O_3$ catalyst with K was found to promote the formation of CO, while methane formation was favored over the unmodified catalyst [56]. Potassium-promoted Fe-based [57] and Fe-Ni bimetallic [58] catalysts were found to be highly active for the $CO_2$ hydrogenation toward lower ($C_2-C_4$) olefins, whereas Li-, Na- and K-promoted Rh-Co/$SiO_2$ catalysts favored ethanol formation via $CO_2$ hydrogenation, with Na being the most effective promoter [59]. Moreover, the nature of the support employed influences the effect of K addition on the $CO_2$ methanation rate, which was found to be lower with the addition of K on Ni/$SiO_2$ and higher for low K contents on Ni/$SiO_2$-$Al_2O_3$ [47]. Interestingly, although $TiO_2$-supported catalysts seem to be promising candidates for the $CO_2$ hydrogenation reaction, the investigations made so far for the modification of $TiO_2$ are limited for the title reaction.

In our recent study, it has been found that $Ru/TiO_2$ catalysts exhibit high activity and selectivity for the $CO_2$ methanation reaction, which can be significantly increased with increasing Ru loading and crystallite size in the range of 0.5–5.0 wt.% and 0.9–4.2 nm, respectively [30]. Moreover, previous studies have shown that small amounts (0.0–0.4 wt.%) of alkali metals are able to improve the activity of various supported catalysts for the WGS reaction [60–68], which as discussed above plays a crucial role in the $CO_2$ methanation pathway. Thus, in the present study, the effect of alkali promotion of $TiO_2$ on the $CO_2$ methanation activity and selectivity of dispersed Ru catalysts has been investigated over 0.5 wt.% Ru/X-$TiO_2$ samples of variable promoter type (X = Li, Na, K, Cs) and loading (0.0–0.4 wt.%). The objective is (a) to investigate the promoting effects of alkalis (Li, Na, K, Cs) on the $CO_2$ methanation activity of $Ru/TiO_2$ catalysts, (b) to develop novel catalytic materials able to selectively convert carbon dioxide to methane and (c) to decrease the amount of precious metal required for $CO_2$ hydrogenation to occur. Moreover, in order to check if the promotion effect of alkalis is also operable over large Ru crystallites, resulting in further activity improvement of $5\%Ru/TiO_2$ catalyst, the effect of sodium loading on catalytic performance of $5\%Ru/Na\text{-}TiO_2$ catalysts has been examined. The alkali-induced modifications of catalytic activity and selectivity are discussed with respect to Ru loading (or crystallite size).

## 2. Experimental

### 2.1. Catalyst preparation and characterization

The addition of alkalis on $TiO_2$ was carried out by impregnation of commercial $TiO_2$ (Aeroxide P25) powder with an aqueous solution of the corresponding alkali precursor salt ($Li_2CO_3$, $NaNO_3$, $KNO_3$ or $CsNO_3$ (Alfa Aesar)) [69]. Typically, the desired amount of the salt was diluted in 50 mL of water, at natural solution pH, followed by addition of 5 g of $TiO_2$ under continuous stirring. The resulting slurry was heated slowly at 70 °C under continuous stirring and maintained at that temperature until nearly all the water evaporated. The solid residue of the alkali-promoted $TiO_2$ supports was dried at 110 °C overnight followed by

**Table 1**
Physicochemical characteristics of the synthesized Ru/X-$TiO_2$ catalysts and their apparent activation energies for $CO_2$ hydrogenation reaction.

| Catalyst | Metal dispersion[a] (%) | Mean metal crystallite size[a] (nm) | Anatase content[b] (%) | $d(TiO_2)$[c] (nm) | Activation Energy (kJ/mol) |
|---|---|---|---|---|---|
| $0.5\%Ru/TiO_2$ | 46.0 | 2.1 | 48 | 23 | 55.6 |
| $0.5\%Ru/0.2\%Cs\text{-}TiO_2$ | 50.2 | 1.9 | 31 | 24 | 60.7 |
| $0.5\%Ru/0.2\%K\text{-}TiO_2$ | 53.5 | 1.8 | 64 | 24 | 59.8 |
| $0.5\%Ru/0.2\%Li\text{-}TiO_2$ | 34.2 | 2.8 | 9 | 29 | 62.8 |
| $0.5\%Ru/0.06\%Na\text{-}TiO_2$ | 43.8 | 2.2 | 52 | 23 | 55.6 |
| $0.5\%Ru/0.2\%Na\text{-}TiO_2$ | 42.0 | 2.3 | 55 | 26 | 56.9 |
| $0.5\%Ru/0.4\%Na\text{-}TiO_2$ | 43.6 | 2.2 | 60 | 23 | 60.2 |
| $5.0\%Ru/TiO_2$ | 23.0 | 4.2 | 47 | 22 | 56.9 |
| $5.0\%Ru/0.2\%Na\text{-}TiO_2$ | 25.5 | 3.7 | 54 | 24 | 62.3 |
| $5.0\%Ru/0.4\%Na\text{-}TiO_2$ | 19.5 | 4.9 | 59 | 27 | 62.3 |

[a] Metal dispersion and mean crystallite size of dispersed Ru crystallites estimated from selective chemisorption of CO at room temperature.
[b] $TiO_2$ phase composition estimated from integral intensities of the anatase (101) and rutile (110) XRD reflections.
[c] Primary crystallite size of $TiO_2$, estimated from XRD line broadening.

calcination in air at 600 °C for 3 h. The concentration of alkalis of the carriers thus prepared was 0.20 wt.% for Cs, K and Li and varied in the range of 0.0–0.40 wt.% for Na (Table 1).

Ruthenium supported catalysts were prepared employing the wet impregnation method with the use of $Ru(NO)(NO_3)_3$ (Ru 1.5% w/v, Alfa Aesar) as metal precursor salt and the above promoted $TiO_2$ powders as supports [30]. Typically, 2 g of alkali-promoted $TiO_2$ was added under continuous stirring in 20 mL of water containing the desired amount of the $Ru(NO)(NO_3)_3$. The resulting slurry was heated slowly at 70 °C under continuous stirring and maintained at that temperature until nearly all the water evaporated. Catalyst synthesis is followed by drying at 110 °C for 24 h and then reduction at 400 °C in $H_2$ flow for 2 h, prior to storage of the samples at atmospheric conditions. The catalysts were further exposed to hydrogen flow at 300 °C in situ, prior to any use. The nominal metal loading of the catalysts thus prepared was 0.5 and 5.0 wt%. All chemicals used for both carriers and catalysts synthesis are of ultra-high purity (99.99%).

The specific surface area of carriers and catalysts was measured employing nitrogen physisorption at 77 K (BET method). The anatase-to-rutile content of $TiO_2$ as well as the primary crystallite size of $TiO_2$ ($d_{TiO2}$) were determined with the use of X-ray diffraction (XRD). Ruthenium dispersion and crystallite size were estimated employing selective chemisorption of CO at room temperature. The structural characteristics of selected catalysts were also investigated employing Transmission Electron Microscopy (TEM) following standard procedures [16,70]. The equipment, methods and procedures used for catalyst characterization are described in detail in the SI.

### 2.2. Catalytic performance tests and kinetic measurements

Catalytic performance tests and kinetic measurements for the $CO_2$ hydrogenation reaction were carried out in the temperature range of 170–450 °C using an apparatus, which is described in the SI. The mass of catalyst used in these experiments was typically 100 mg (particle size: $0.18 < d_p < 0.25$ mm), the total flow rate was 150 $cm^3\ min^{-1}$, whereas the feed stream was consisted of 5%$CO_2$ + 20%$H_2$ (in He). The gas hourly space velocity (GHSV) used in these experiments was 56000 $h^{-1}$. Prior to each experiment the catalyst was reduced *in situ* at 300 °C for 1 h under 50%$H_2$/He flow (60 $cm^3\ min^{-1}$). Reaction gases (He, $CO_2$, $H_2$) are supplied from high-pressure gas cylinders (Air Products, Sol Group) and are of ultra-high purity (99.99%). Conversion of reactants and selectivities toward products were determined at steady-state conditions using a gas-chromatograph (Shimadzu) and employing the procedures described in detail in the SI.

Carbon dioxide conversion ($X_{CO2}$) was calculated using the following expression:

$$X_{CO_2} = \frac{C_{CO_2,in}\cdot F_{in} - C_{CO_2,out}\cdot F_{out}}{C_{CO_2,in}\cdot F_{in}} \times 100 \quad (3)$$

where $C_{CO_2}$,*in* and $C_{CO_2}$,*out* are the concentrations of $CO_2$ in the inlet and outlet of the reactor, respectively, and $F_{in}$ and $F_{out}$ are the total flow rates ($cm^3\ s^{-1}$) in the inlet and outlet of the reactor, respectively.

Selectivities t○ward $CH_4$ ($S_{CH4}$) and CO ($S_{CO}$) were calculated according to the expressions:

$$S_{CO} = \frac{C_{CO,out}}{C_{CO,out} + C_{CH_4,out}} \times 100 \quad (4)$$

$$S_{CH4} = \frac{C_{CH4,out}}{C_{CO,out} + C_{CH_4,out}} \times 100 \quad (5)$$

where $C_{CH_4,out}$and $C_{CO,out}$ are the outlet concentrations of $CH_4$ and CO, respectively.

Measurements of reaction rates were obtained in separate experiments under differential reaction conditions, where the conversion of carbon dioxide was kept below 10%.

Experimental conditions used were identical with those described above, with the exception of the total flow rate and/or the mass of catalyst, which were appropriately varied in order to ensure that $X_{CO2}$ was kept lower than 10% over a wide temperature range. In particular, GHSV was varied in the range of 28000–60000 $h^{-1}$.

Rates were calculated using the following expression:

$$r_{CO_2} = \frac{C_{CO_2,in}\cdot F_{in} - C_{CO_2,out}\cdot F_{out}}{W} \quad (6)$$

where $r_{CO_2}$ is the conversion rate of $CO_2$ (mol $s^{-1}$ $g_{cat}{}^{-1}$), $F_{in}$ and $F_{out}$ are the total flow rates in the inlet and outlet of the reactor ($cm^3\ s^{-1}$), respectively, $W$ is the mass of catalyst and, $C_{CO_2,in}$, $C_{CO_2,out}$are the inlet and outlet concentrations of $CO_2$, respectively.

The turnover frequencies (TOFs) of carbon dioxide conversion, defined as moles of $CO_2$ converted per surface ruthenium metal atom per second ($s^{-1}$), were calculated using the results obtained from reaction rate measurements and metal dispersions:

$$TOF = \frac{r_{CO_2}\cdot AW_{Ru}}{D\cdot X_{Ru}} \quad (7)$$

where $AW_{Ru}$ (=101.07 g/mol) is the atomic weight of Ru, $X_{Ru}$ is the metal content ($g_{Pt}/g_{cat}$) and $D$ is the Ru dispersion.

## 3. Results and discussion

### 3.1. Catalyst characterization

Results of nitrogen physisorption measurements showed that the specific surface area is not influenced by addition of small amounts of alkalis on the $TiO_2$ support, taking practically the same values for all catalysts investigated (27–30 $m^2\ g^{-1}$). This is also the case upon dispersion of Ru on the support surface.

The X-ray diffractograms obtained from the synthesized 0.5% and 5.0%Ru/X-$TiO_2$ catalysts are shown in Fig. 1. It is observed that, all samples consist of $TiO_2$ in both its anatase and rutile form. The anatase content increases progressively with increasing Na loading for both 0.5%Ru and 5%Ru/Na-$TiO_2$ catalysts. The mean primary crystallite size of $TiO_2$, estimated from X-ray peak broadening, is not affected significantly by the presence of the promoters and varies in the range of 23–29 nm for all samples investigated (Table 1).

Results of CO chemisorption measurements are summarized in Table 1, where it is observed that both ruthenium dispersion and mean crystallite size are not influenced significantly by alkali addition on $TiO_2$ support. In the case of 0.5%Ru/X-$TiO_2$ catalysts, Ru dispersion and crystallite size vary in the range of 34.2–53.5% and 1.8–2.8 nm, respectively. The dispersion of 5.0%Ru/Na-$TiO_2$ catalysts is, in general, lower, taking values between 19.5 and 25.5%, whereas the mean crystallite size of Ru is higher, varying between 3.7 and 4.9 nm.

The structural characteristics of selected catalysts were also investigated by TEM. Representative TEM images obtained from 0.5%Ru/$TiO_2$, 0.5%Ru/0.2%Na-$TiO_2$, 5%Ru/$TiO_2$ and 5%Ru/0.2%Na-$TiO_2$ catalysts are presented in Fig. 2. It is observed that ruthenium crystallites are hard to be discerned in the case of 0.5%Ru/$TiO_2$ (Fig. 2A) and 0.5%Ru/0.2%Na-$TiO_2$ catalysts (Fig. 2B), most probably due to their small size and thus, their diameter was hard to be estimated. Fig. 2C and D showed that 5%Ru/$TiO_2$ and 5%Ru/0.2%Na-$TiO_2$ catalysts comprise fairly homogeneously dispersed spherical Ru particles of approximately 4.0 and 3.7 nm diameter, respectively. Results indicate that the shape and the size of catalysts particles do not change by addition of alkalis. Ruthenium crystallite sizes obtained by TEM analysis agree well with those estimated based on CO chemisorption measurements (Table 1).

### 3.2. Thermodynamic analysis of $CO_2$ hydrogenation reaction

Thermodynamic analysis of the $CO_2$ hydrogenation reaction has been carried out using the Outokumpu HSC Chemistry® program. The

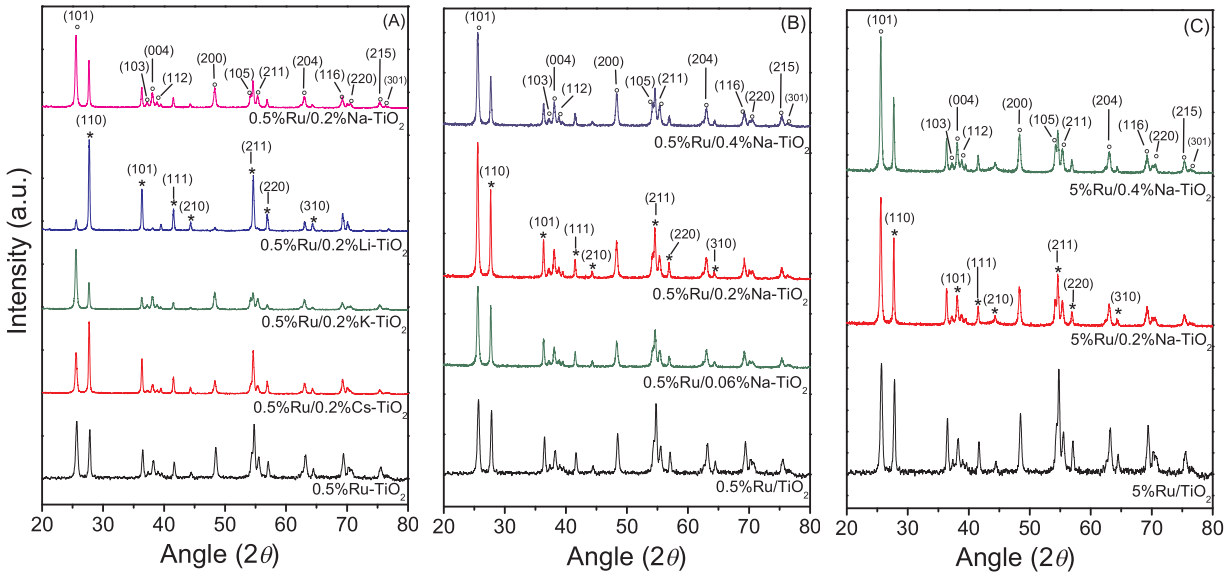


**Fig. 1.** X-ray diffractograms of (A) 0.5%Ru/0.2%X-$TiO_2$, (B) 0.5%Ru/Na-$TiO_2$ of variable Na content and (C) 5%Ru/Na-$TiO_2$ of variable Na content. The reflection planes of anatase (°) and rutile(*) phases are indicated.

changes of Gibbs free-energy ($\Delta G_0{}^T$) and enthalpy ($\Delta H_0{}^T$) of the reaction were calculated as functions of reaction temperature. It was found that the reaction is exothermic, with $\Delta H_0{}^T$ decreasing from −163.5 to −189.2 kJ $mol^{-1}$, with increasing temperature in the range of 0–700 °C (Fig.S1A). The Gibbs free-energy takes positive values at temperatures higher than 600 °C, indicating that the reaction is not favored thermodynamically above that temperature (Fig.S1A). The equilibrium constant was determined as a function of temperature (Fig.S1B) and was used to calculate the equilibrium conversion of $CO_2$ as a function of temperature (dashed line presented in Figs. 3 A, 5 A and 8 A) for the feed composition used in the present study (5% $CO_2$ + 20% $H_2$ in He). Results obtained are in good agreement with those reported in the literature [27,71].

### 3.3. Effect of alkali additives on the catalytic performance of 0.5%Ru/$TiO_2$ catalyst

The effect of alkali promotion on the catalytic performance of 0.5% Ru/$TiO_2$ catalyst was investigated over samples containing 0.2 wt.% Li, Na, K or Cs. Results obtained are presented in Fig. 3A, where the $CO_2$ conversion ($X_{CO2}$) is plotted as a function of reaction temperature. The equilibrium conversion, predicted by thermodynamics, is also shown

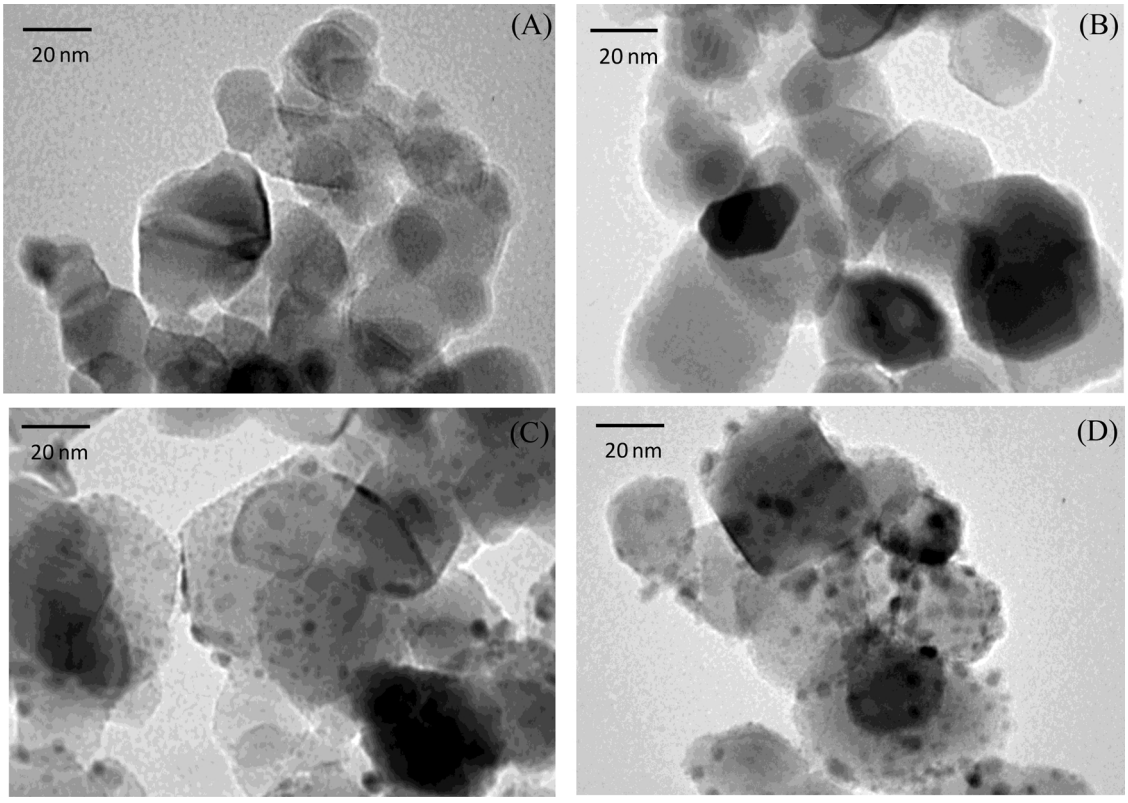


**Fig. 2.** TEM images of (A) 0.5%Ru/$TiO_2$, (B) 0.5%Ru/0.2%Na-$TiO_2$ (C) 5%Ru/$TiO_2$ and (D) 5%Ru/0.2%Na-$TiO_2$ catalysts.

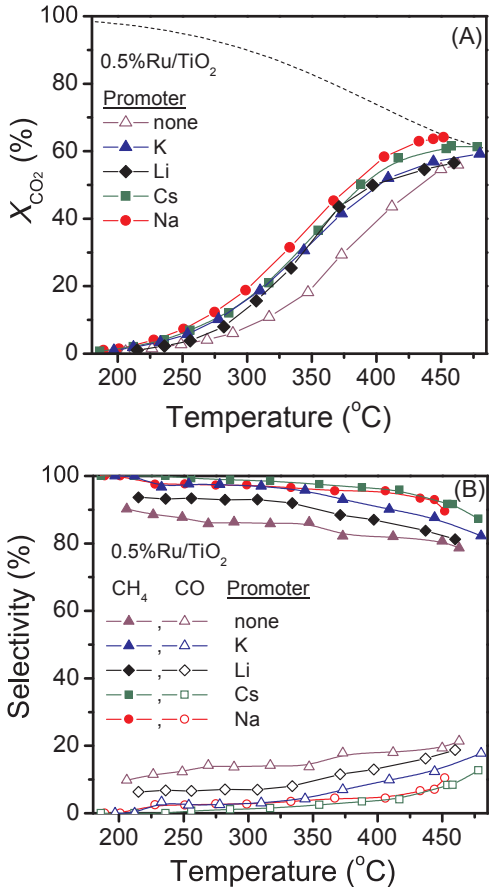


**Fig. 3.** (A) Conversions of $CO_2$ and (B) selectivity toward $CH_4$ and CO as a function of reaction temperature obtained over alkali-promoted 0.5%Ru/X-$TiO_2$ catalysts of the same alkali loading (0.2 wt.%). Experimental conditions: Mass of catalyst: 100 mg; particle diameter: $0.18 < d_p < 0.25$ mm; Feed composition: 5%CO, 20% $H_2$ (balance He); Total flow rate: 150 $cm^3\ min^{-1}$.

for comparison (dashed line). It is observed that the unpromoted 0.5% Ru/$TiO_2$ catalyst is activated at around 230 °C, whereas temperatures higher than 460 °C are required to achieve equilibrium $CO_2$ conversions. The catalytic performance of Ru is significantly improved with the addition of 0.2 wt.% of alkalis on $TiO_2$. Optimum results have been obtained over the Na-promoted catalyst, the conversion curve of which is shifted toward lower temperatures (by about 60 °C), compared to that of the unpromoted catalyst.

In Fig. 3B are presented the selectivities toward reaction products as a function of reaction temperature for the alkali-promoted catalysts investigated. In all cases, $CO_2$ hydrogenation results in the production of $CH_4$ and CO, the distribution of which depends on the catalyst employed. In the case of the unpromoted sample, the selectivity toward methane ($S_{CH4}$) decreases from 90 to 79% with increasing temperature from 200 to 470 °C, whereas the selectivity toward CO ($S_{CO}$) increases from 10 to 21%. The same trend was observed with respect to reaction temperature upon addition of alkalis. However, alkali promotion results in an increase of methane selectivity in a manner which depends on the nature of alkali additive. In particular, $S_{CH4}$ at a given temperature increases following the order $TiO_2$ (unpromoted) < Li < K < Cs ~ Na.

The relative experimental error of data points was calculated taking into account the scatter on the data at each reaction temperature. Results showed that the relative experimental error was lower than 0.6%, which is minor compare to the observed increase of both $X_{CO2}$ and $S_{CH4}$ upon alkali addition.

In our previous works, a detail mechanistic study of the $CO_2$ hydrogenation reaction was carried out over 0.5% and 5.0%Ru/$TiO_2$ catalysts employing in situ FTIR and transient mass spectrometry (transient-MS) techniques [15,16,23,30]. DRIFT experiments showed that interaction of the catalyst surface with $CO_2/H_2$ mixture at low temperatures results in the development of bands due to carbonate and formate species associated with $TiO_2$ support. The relative population of the latter species started decreasing at higher temperatures, where ruthenium-bonded carbonyl species started to be developed. Thus, it has been suggested that hydrogen adsorbed on Ru surface is diffused at the metal-support interface where it reacts with $CO_2$, which is mainly adsorbed on $TiO_2$, yielding formate and, eventually, adsorbed CO species (RWGS). Part of the produced carbonyl species was found to interact with adsorbed hydrogen atoms leading to evolution of methane, whereas the remaining produced CO cannot be further hydrogenated to methane and was desorbed in the gas phase. The relative rate of these pathways, which depends on experimental conditions and catalyst employed, determines selectivity toward $CH_4$ or CO. Based on these findings and taking into account that selectivity toward methane is enhanced over alkali-promoted catalysts (Fig. 3B), following a monotonic trend with respect to catalytic activity, it can be suggested that hydrogenation of intermediate produced CO species is enhanced compared to its desorption in the gas phase upon alkali addition.

Results of specific reaction rates measured over the 0.5%Ru/0.2%X-$TiO_2$ catalysts under differential reaction conditions are summarized in the Arrhenius diagram of Fig. 4. In all cases, the relative experimental error of reaction rate measurements was found to be lower than 0.6%. It is observed that the TOF of $CO_2$ conversion is higher over the alkali-containing samples and depends on the nature of the promoter. Specific activity follows the order $TiO_2$ (unpromoted) < Li ~ K < Cs < Na, with the Na-promoted sample being around 3 times more active at 250 °C compared to the unpromoted 0.5%Ru/$TiO_2$. The beneficial effect of sodium promoter on $CO_2$ hydrogenation activity has been also reported over 5%Ru/$Al_2O_3$ [54] and Rh-Co/$SiO_2$ [59] catalysts, and has been attributed to the improvement of $CO_2$ adsorption capacity and to an increase of the population of reactive surface species for $CO_2$ hydrogenation, respectively.

In our previous study, it has been found that $CO_2$ hydrogenation reaction is structure sensitive with respect to the metal, i.e., catalytic activity is strongly influenced by metal crystallite size. In the case of Ru/$TiO_2$ catalysts, the TOF increases by two orders of magnitude with increasing ruthenium crystallite size in the range of 0.9–4.2 nm [30]. However, the size of Ru particles of the alkali-promoted catalysts presented in Fig. 4 varies in the narrow range of 1.8–2.8 nm (Table 1), without presenting any trend with respect to catalytic activity. This indicates that the observed increase of TOF cannot be attributed to crystallite size effect.

The apparent activation energy ($E_a$) of the $CO_2$ hydrogenation reaction was calculated from the slopes of the fitted lines shown in Fig. 4

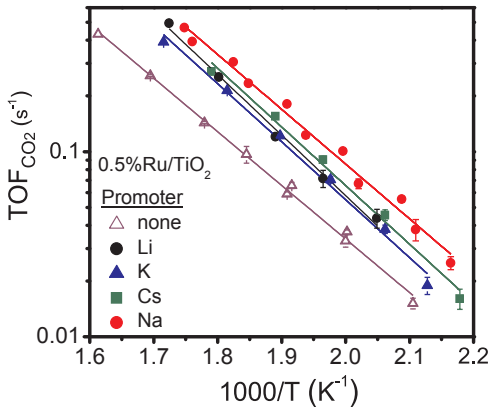


**Fig. 4.** Arrhenius plots of turnover frequencies of $CO_2$ conversion obtained over alkali-promoted 0.5%Ru/X-$TiO_2$ catalysts of the same alkali loading (0.2 wt.%). Experimental conditions: same as in Fig. 3.

and results are summarized in Table 1. It is observed that $E_a$ is not affected appreciably by added alkali (Table 1), increasing slightly from 55.6 to 62.8 kJ $mol^{-1}$. This implies that the presence of the promoters does not change either the reaction mechanism or the rate limiting step. However, it should be mentioned that two reactions, $CO_2$ methanation and RWGS, run simultaneously under the present conditions, each one of which depends in a different manner on temperature and alkali promotion. Thus, the estimated value of $E_a$ arises from both reactions, the contribution of which to the activation energy with respect to alkali promotion cannot be accurately clarified. Results are in agreement with previous studies over supported Ni catalysts, where it was found that the activation energy for the $CO_2$ methanation reaction does not depend strongly on K promotion [47].

It is of interest to note that most of the studies reported so far on the effect of alkali promotion for the $CO_2$ hydrogenation reaction are mainly related to potassium addition, which in most cases suppresses the $CO_2$ methanation activity [2,46,47,56,72–75]. For example, Büchel et al. [2] found that the K-containing $Rh/Al_2O_3$ catalysts promote $CO_2$ conversion entirely to CO, whereas no methane formation was observed. Similar results have been obtained over K-promoted Pt/mullite [73], Fe-Al-O spinel [75], $Fe_5C_2$ [75] and $Ni/CeO_2$ [74] catalysts. In the latter case, the methane-suppressing effect of potassium has been attributed to the formation of adsorbed bridging carbonyls, at the expense of subcarbonyl nickel species $Ni(CO)_n$ (n = 2 or 3), which was found to be methane precursors. Moreover, strong adsorption of CO in the bridging mode prevents CO dissociation and hydrogenation of surface carbon, resulting in low methane yield. Heyl et al. [56] investigated the $CO_2$ methanation mechanism over K modified $Rh/Al_2O_3$ catalysts and demonstrated that hydrogen dissociation ability as well as the adsorption strength of CO are affected by the presence of K, which favors the desorption of the intermediate produced CO from the catalyst surface and hinders CO hydrogenation to methane. Moreover, potassium was found to be unable to methanate $CO_2$, but was a key promoter for alkene and ethanol formation over Fe catalyst supported on N-functionalized carbon nanotubes [72].

To our knowledge, only a few studies, related to alkali promotion, reported improved catalytic activity for the $CO_2$ hydrogenation reaction [47,50,51,53,54]. For example, Campbell et al. [47] found that low K loadings (< 1 wt.%) over $Ni/SiO_2$-$Al_2O_3$ catalysts resulted in higher $CO_2$ hydrogenation rates compared to the unpromoted sample. An increase of $CO_2$ methanation activity was recently reported over Cu-K/$Al_2O_3$ catalysts and was assigned to enhancement of $CO_2$ adsorption, due to decrease of surface acidic sites induced by K addition [50]. The increase of $CH_4$ selectivity against to CO selectivity was related to the electron donor character of potassium, which controls CO adsorption by interacting with Cu and thus, enhancing $CO_2$ conversion to methane. A similar suppression of CO production was recently reported by Kalaitzidou et al. [51] for the electrochemical promotion of $CO_2$ to $CH_4$ and CO over Ru catalyst-electrodes deposited on $Na^+$ and $K^+$ conducting ceramic supports. It should be noted that the observed differences between literature and results of the present study may be attributed to the different catalyst preparation method employed, the different metal-support combinations and/or, as it will be discussed below, to the different metal loading and crystallite size, which strongly affects catalytic activity for the title reaction [30].

In our previous studies [61,69], the effects of alkali additives on the physicochemical characteristics and chemisorptive properties of $TiO_2$-supported noble metal catalysts have been investigated with the use of diffuse reflectance infrared spectroscopy (DRIFTS). Results showed that addition of alkalis results in the development of a new, low frequency band, which increases in intensity and shifts toward lower frequencies with increasing alkali concentration, indicating the strengthening of the M-CO bond. The low frequency of this band indicated the presence of adsorption sites of exceptional electron-donating properties. It has been proposed that these sites are located at the perimeter of the dispersed metal crystallites, which are in contact with the alkali-modified $TiO_2$ support. Modification of support properties and creation of new active sites by alkali addition was also reported by Pazmiño et al. [68]. Since $CO_2$ methanation reaction proceeds via intermediate formation of CO at the metal support-interface via the RWGS reaction, it is possible that added alkalis affect the nature, the population and/or the adsorption strength of Ru-carbonyl intermediates, resulting in enhancement of catalytic activity in a manner which depends on the type and, as it will be shown below, the loading of the promoter. It should be noted, that the addition of alkali metals has been shown to improve the activity of various supported catalysts for the WGS reaction [60–68], which plays a crucial role in the $CO_2$ methanation pathway.

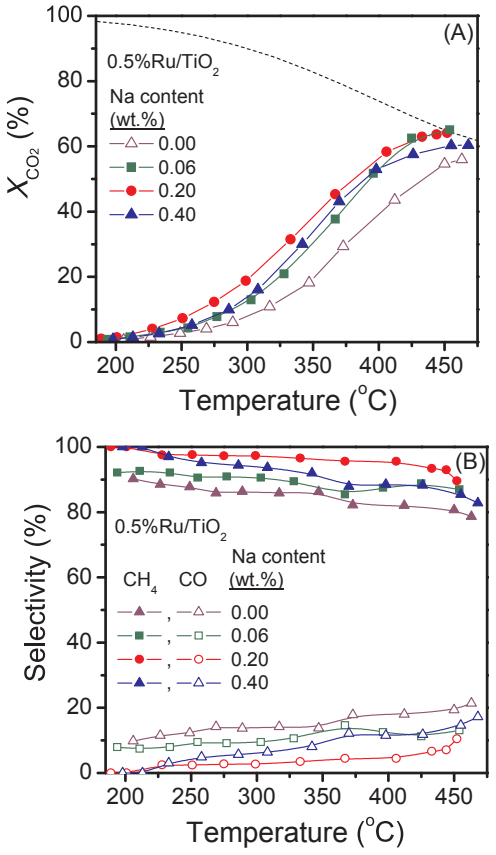


**Fig. 5.** (A) Conversion of $CO_2$ and (B) selectivity toward $CH_4$ and CO obtained over sodium-promoted 0.5%Ru/$TiO_2$ catalysts of variable sodium loadings (wt.%). Experimental conditions: same as in Fig. 3.

### 3.4. Effect of sodium loading on the catalytic performance of 0.5%Ru/$TiO_2$ catalyst

The effect of alkali loading on catalytic activity and selectivity has been investigated over 0.5%Ru/Na-$TiO_2$ catalysts of variable Na content. Results obtained (Fig. 5A) show that the $CO_2$ conversion curve shifts progressively toward lower temperatures with increasing Na content from 0.0 to 0.2 wt.%, whereas further increase of Na content to 0.4 wt.% has the opposite effect. In particular, the 0.5%Ru/0.4%Na-$TiO_2$ catalyst exhibits similar performance with that of 0.5%Ru/0.06% Na-$TiO_2$.

The effect of sodium loading on the selectivities toward methane and carbon monoxide are summarized in Fig. 5B, where it is observed that $S_{CH4}$ at a given temperature increases with increasing Na content in the range of 0.0–0.2 wt.%, followed by a decrease of $S_{CO}$. Further increase of Na loading to 0.4 wt.% results in lower $CH_4$ and higher CO selectivities compared to that of the 0.5%Ru/0.2%Na-$TiO_2$ catalyst, indicating that there is an optimum Na content which enhances methanation of $CO_2$. However, in all cases the sodium- promoted catalysts

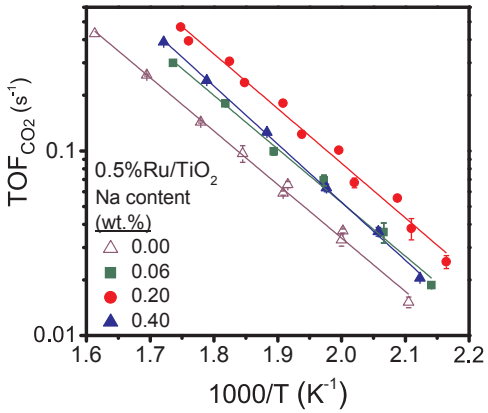


**Fig. 6.** Arrhenius plots of turnover frequencies of $CO_2$ conversion obtained over sodium-promoted 0.5%Ru/$TiO_2$ catalysts of variable sodium loadings (wt.%). Experimental conditions: same as in Fig. 3.

exhibit higher methane selectivities compared to that of the unpromoted sample. It should be noted that the increase of both catalytic activity and methane selectivity was not within the experimental error limits (0.1–0.6%).

The Arrhenius-type diagram of Fig. 6 shows the results of reaction rate measurements obtained over Na-promoted 0.5%Ru/$TiO_2$ catalyst. It is observed, that the specific activity increases with increasing Na content up to 0.2 wt.% and decreases upon further increasing sodium concentration. This behavior is clearly depicted in Fig. 7A, where the TOF at 250 °C is plotted as a function of Na content. Turnover frequency goes through a maximum for 0.2 wt.% Na, exhibiting an increase by a factor of 2.6 compared to the unpromoted sample. Selectivity toward $CH_4$ at 250 °C presents a similar variation with Na loading, taking a maximum value of 98% for the 0.5%Ru/0.2%Na-$TiO_2$ sample, whereas

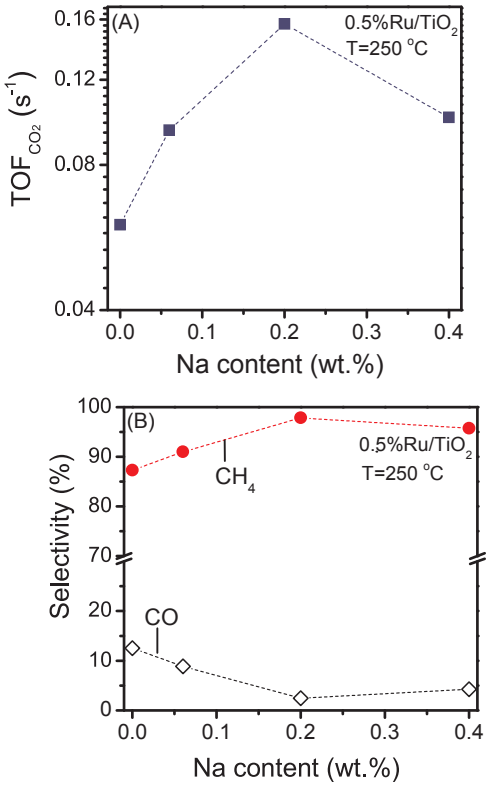


**Fig. 7.** Effect of sodium loading (wt.%) on the (A) turnover frequencies of $CO_2$ conversion and (B) selectivity toward $CH_4$ and CO obtained at 250 °C over 0.5%Ru/$TiO_2$ catalysts. Experimental conditions: same as in Fig. 3.

the opposite trend is observed for CO selectivity (Fig. 7B). A similar volcano-type dependence of $CO_2$ methanation activity on promoter loading has been observed over K- and Cs-promoted Ru/$Al_2O_3$ [54], where the reaction rate was found to increase by a factor 2.2 and 2.8, respectively. The authors found that the optimum amount of alkali additives depended on the alkali type and was achieved by covering the catalyst surface by alkali metal atoms with an approximate monolayer state. Similarly, Campbell et al. [47] found that the turnover number of methane formation of K-promoted Ni/$SiO_2$-$Al_2O_3$ catalysts increased from 3.2 to 4.3 $s^{-1}$ with increasing K content from 0 to 0.81 wt.%, followed by a decrease of the turnover number of CO formation. However, the methanation rate decreased to 4.1 $s^{-1}$ with further increasing K loading to 3.9 wt.%, while the CO turnover number increased by more than one order of magnitude. According to the authors, this behavior was due to the preferential interaction of potassium with the acid sites of $SiO_2$-$Al_2O_3$ support, which was enhanced for low promoter loadings, where most of the potassium was located on the surface of the support and was able to modify the reaction properties of the promoter [47]. It should be noted, however, that this interpretation cannot be used to explain the volcano-type behavior of Fig. 7, since the nature of the metallic phase, the support and the promoter employed are different than those reported by Campbell et al. [47]. Comparison of the specific activities observed over K-promoted Ni/$SiO_2$-$Al_2O_3$ catalysts with those presented in Fig. 7 shows that the effect of Na loading on TOF is significantly higher for the Ru/$TiO_2$ catalysts of the present study.

It is of interest to note that Ru crystallite size remains practically constant with increasing Na content, taking values between 2.1 and 2.3 nm (Table 1). This indicates that the size of metal crystallites is not influenced by the presence of the promoter and that the increased TOF observed in Figs. 6 and 7 is not related to the structure sensitivity of the reaction.

Our previous studies, on the WGS reaction over alkali-promoted Pt/$TiO_2$, Ru/$TiO_2$ and Pd/$TiO_2$ catalysts, clearly indicated the absence of a strong electronic effect of alkali additives on the adsorption strength of sites located on the surface of metal, in agreement with results reported by Pazmiño et al. [68]. In contrast, it was found that increasing Na or Cs loading results in an increase of the number of sites at the metal-support interface and in a monotonic increase of their adsorption strength toward CO [61,68,69]. The WGS reaction was found to be favored over materials with intermediate CO heat of adsorption and thus, the specific reaction rate exhibited a maximum value for catalysts with intermediate alkali content [61,76]. In the case of Ru/$TiO_2$ catalysts the optimum WGS activity was obtained for the catalyst containing 0.2 wt.% Na [61], which also exhibited the optimum $CO_2$ methanation activity in the results of the present study (Fig. 7A). Since the conversion of $CO_2$ toward CO, via the RWGS reaction, is the initial step on the $CO_2$ methanation pathway, it is possible that the population and the adsorption strength of the produced carbonyl species are optimized for the 0.5% Ru/0.2% Na-$TiO_2$ catalyst. If this is the case, then the intermediate produced CO is expected to be stronger adsorbed on the surface of the latter catalyst compared to the unpromoted sample, favoring dissociation of CO and subsequent hydrogenation of surface carbon to methane, rather than CO desorption in the gas phase. Higher sodium concentrations may results in lower RWGS activity and therefore, lower population of reactive carbonyl species for hydrogenation toward methane.

The ability of alkali additives to modify the chemisorptive properties of catalysts with respect to CO can be understood by considering that alkali metals are electron donors and, when present on the catalyst surface, results in electron transfer toward metal, which increases the back-donation of the metal electrons into the $2\pi^*$ antibonding orbitals of adsorbed CO [77–82]. Thus, alkali additives result in strengthening of the metal-CO (M-CO) bond and weakening of the carbon-oxygen (C—O) bond. Such strongly bound CO species have been detected on the surface of Ru/$SiO_2$ catalyst with increasing potassium content [78]. The

alkali-induced dissociation of CO has been previously observed over Fe [83], Ni [84,85], Co [86], Ru [45,78] and Pt [87] catalysts. Kiskinova et al. [84] reported that addition of electropositive elements, such as Na, K or Cs, strongly enhances the dissociative adsorption of CO, the fraction of which was found to increase with the amount of alkali adatoms present, favoring hydrogenation of surface carbon to $CH_4$.

Regarding the apparent activation energy of the reaction, results show that Ea varies in the short range of 55.6–60.2 kJ/mol for catalysts of variable Na loading (Table 1). This agrees well with previous studies over K-promoted $Pt/SiO_2$ [87], $Ni/SiO_2$ [47] and $Ni/SiO_2$-$Al_2O_3$ [47] catalysts, where it was found that there was no significant effect of K-promotion on activation energy.

It should be noted that results of the present study cannot be used to explain the origin of the alkali-induced improvement of the $CO_2$ methanation activity. Clearly, detailed mechanistic studies are necessary to further investigate the effect of alkali promotion on the $CO_2$ methanation pathway, which will be the subject of our subsequent publication.

### 3.5. Effect of sodium loading on the catalytic performance of 5%Ru/$TiO_2$ catalyst

In our recent study, it has been found that $CO_2$ methanation reaction is structure sensitive with respect to the metal, i.e., catalytic activity is strongly influenced by metal crystallite size [30]. In the case of $Ru/TiO_2$ catalysts, the intrinsic reaction rate increases by two orders of magnitude with increasing ruthenium loading and crystallite size in the range of 0.5–5.0 wt.% and 0.9–4.2 nm, respectively.

In order to check if the promotion effect of alkalis is also operable over large Ru crystallites, the effect of sodium loading on catalytic performance has been examined over 5%$Ru/TiO_2$ catalyst. As in the case of low Ru loading, Ru crystallite size of this set of catalysts was not influenced significantly by the presence of alkalis, taking values in the range of 3.7–4.9 nm (Table 1). Sodium content was varied between 0.0 and 0.4 wt.% and results obtained are summarized in Fig. 8. The conversion curve of $CO_2$ shifts toward lower temperatures upon Na addition, with the effect being more pronounced at temperatures higher than 250 °C. As in the case of 0.5%$Ru/TiO_2$ catalysts, the sample containing 0.2 wt.% Na exhibits the optimum performance (Fig. 8A). Comparison of Figs. 5A and 8A shows that $X_{CO2}$ of Ru/0.2%Na-$TiO_2$ catalysts increases (e.g. from 55 to 80% at 300 °C) with increasing Ru loading from 0.5 to 5.0 wt.%. A qualitatively similar increase of $CO_2$ conversion was reported by Ahmad et al. [50], who found that $X_{CO2}$ of Cu-0.5%$K/Al_2O_3$ catalysts increases from 17.2 to 28.3% at 400 °C with increasing Cu content from 1 to 1.62 wt.%, respectively.

Selectivity toward methane is almost 100% for all the (promoted or not) 5%$Ru/TiO_2$ catalysts investigated, whereas only traces of CO can be detected (Fig.S2). In our previous study, it was found that, for $Ru/TiO_2$ catalysts, selectivity toward methane, at a given temperature, increases from 90 to 100% with increasing Ru loading from 0.5 to 5 wt.% (or Ru crystallite size from 2.1 to 4.2 nm) [30]. Since the formation CO is diminished substantially for high ruthenium loadings (or large Ru particles), no significant variations were expected in product distribution over Na-promoted 5%$Ru/TiO_2$ catalysts, which agrees well with results of Fig.S2.

Turnover frequencies calculated for the 5%$Ru/TiO_2$ and 5%Ru/0.4%Na-$TiO_2$ catalysts, practically, lie on the same line, whereas a slight increase of TOF, by a factor of less than 1.2, is observed for the 5%Ru/0.2%Na-$TiO_2$ catalyst (Fig. 8B). This indicates that the specific activity for $CO_2$ hydrogenation reaction over large Ru crystallites is essentially not affected by the presence of sodium on the catalyst surface. Although, the effect of alkali promotion over supported metal catalysts of high metal loading (5 or 10 wt.%) has been examined by several researchers [31,47,54], to our knowledge, no comparison with corresponding results obtained over supported metal catalysts of low metal loading has been reported.

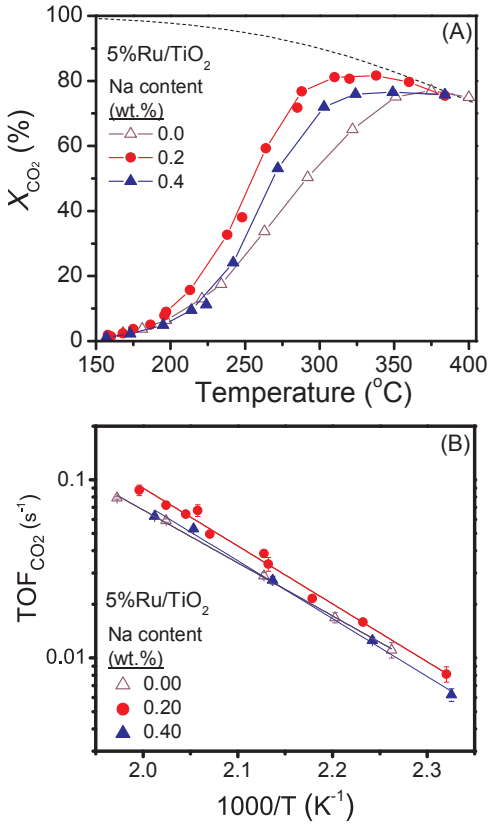


**Fig. 8.** (A) Conversions of $CO_2$ as a function of reaction temperature and (B) Arrhenius plots of turnover frequencies of $CO_2$ conversion of sodium-promoted 5%$Ru/TiO_2$ catalysts of variable sodium loadings (wt.%). Experimental conditions: same as in Fig. 3.

Results of the present study can be explained taking into account that the length of the metal/support interface decreases with increasing metal particle size. In particular, the total perimeter of the metal/support interface per Ru surface area was calculated for $Ru/TiO_2$ catalysts and it was found to be decreased progressively with increasing ruthenium crystallite size from 2.1 to 4.2 nm [30]. If, as suggested above, the enhancement of $CO_2$ methanation activity upon alkali addition is related to the initial step of $CO_2$ conversion toward CO species (RWGS) adsorbed on sites located at the metal/support interface, it is reasonable to suggest that the population of the latter species is limited over catalysts of large Ru particles and therefore, the reaction rate is not significantly affected. Since the $CO_2$ methanation reaction is structure sensitive [16,30], it can then be argued that the effect of Ru crystallite size on catalytic activity predominates compared to the effect of alkali promotion over large Ru crystallites and thus, catalytic activity cannot be further improved. It should be noted, however, that the present results do not provide mechanistic information on the effect of alkali promotion. As mentioned above, detailed mechanistic studies are necessary to elucidate the mechanism of the $CO_2$ methanation reaction over alkali promoted $Ru/TiO_2$ catalysts.

The apparent activation energy is practically independent of Na loading, varying in the narrow range of 56.9–62.3 kJ/mol (Table 1).

Interestingly, comparison of Figs. 6 and 8 B show that the TOF of 0.5%Ru/0.2%Na-$TiO_2$ is higher (by a factor of 1.5), at a given temperature, than that measured over 5%$Ru/TiO_2$ catalyst. This can be clearly seen in Fig.S3 and is of significant practical importance, indicating that a significant part of 5 wt.% Ru content can be replaced by a small amount of Na (0.2 wt.%), resulting in a material of lower cost, able to convert efficiently $CO_2$ to methane.

## 4. Conclusions

The $CO_2$ methanation activity of $Ru/TiO_2$ catalysts can be enhanced significantly by addition of small amounts of alkalis (Li, Na, K, Cs) on the $TiO_2$ support, in a manner which depends appreciably on the nature and loading of the promoter, as well as on the dispersed Ru loading (or Ru crystallite size). In the case of $0.5\%Ru/TiO_2$ catalysts, TOF follows the order $TiO_2$ (unpromoted) < Li ~ K < Cs < Na, with the Na-promoted sample being around 3 times more active compared to the unpromoted catalyst. The same trend is observed for methane selectivity, whereas carbon monoxide selectivity presents the opposite behavior. Specific activity goes through a maximum with increasing sodium content from 0.0 to 0.4 wt.%, with the sample containing 0.2 wt.% Na exhibiting optimum catalytic activity and methane selectivity. The effect of alkali promotion is less pronounced in the case of $5\%Ru/TiO_2$ catalysts, where specific activity was found to increase only slightly upon sodium addition on $TiO_2$. Results provide evidence that addition of alkalis promotes hydrogenation of intermediate produced CO to $CH_4$ over well dispersed Ru particles, whereas large Ru particles do not “feel” the presence of the promoter. The optimized $0.5\%Ru/0.2\%Na\text{-}TiO_2$ catalyst exhibits higher specific activity than that of $5\% Ru/TiO_2$ catalyst and, therefore, is a promising candidate for the $CO_2$ methanation reaction.

## Appendix A. Supplementary data

Supplementary data associated with this article can be found, in the online version, at http://dx.doi.org/10.1016/j.apcatb.2017.11.048.

## References


[1] A. Karelovic, P. Ruiz, Appl. Catal. B: Environ. 113–114 (2012) 237–249.
[2] R. Büchel, A. Baiker, S.E. Pratsinis, Appl. Catal. A: Gen. 477 (2014) 93–101.
[3] M. Jacquemin, A. Beuls, P. Ruiz, Catal. Today 157 (2010) 462–466.
[4] J. Ren, H. Guo, J. Yang, Z. Qin, J. Lin, Z. Li, Appl. Surf. Sci. 351 (2015) 504–516.
[5] A. Westermann, B. Azambre, M.C. Bacariza, I. Graça, M.F. Ribeiro, J.M. Lopes, C. Henriques, Appl. Catal. B: Environ. 174–175 (2015) 120–125.
[6] C. Swalus, M. Jacquemin, C. Poleunis, P. Bertrand, P. Ruiz, Appl. Catal. B: Environ. 125 (2012) 41–50.
[7] X. Wang, H. Shi, J.H. Kwak, J. Szanyi, ACS Catal. 5 (2015) 6337–6349.
[8] S. Akamaru, T. Shimazaki, M. Kubo, T. Abe, Appl. Catal. A: Gen. 470 (2014) 405–411.
[9] M. Iglesias G, C. de Vries, M. Claeys, G. Schaub, Catal. Today 242 (Part A) (2015) 184–192.
[10] A. Beuls, C. Swalus, M. Jacquemin, G. Heyen, A. Karelovic, P. Ruiz, Appl. Catal. B: Environ. 113 (2012) 2–10.
[11] E. Baraj, S. Vagaský, T. Hlinčík, K. Ciahotný, V. Tekáč, Chem. Pap. 70 (2016) 395–403.
[12] I.A. Fisher, A.T. Bell, J. Catal. 162 (1996) 54–65.
[13] G.D. Weatherbee, C.H. Bartholomew, J. Catal. 87 (1984) 352–362.
[14] M. Marwood, R. Doepper, A. Renken, Appl. Catal. A: Gen. 151 (1997) 223–246.
[15] P. Panagiotopoulou, D.I. Kondarides, X.E. Verykios, Catal. Today 181 (2012) 138–147.
[16] P. Panagiotopoulou, X.E. Verykios, J. Phys. Chem. C 121 (2017) 5058–5068.
[17] F. Solymosi, A. Erdöhelyi, T. Bánsági, J. Catal. 68 (1981) 371–382.
[18] X. Wang, Y. Hong, H. Shi, J. Szanyi, J. Catal. 343 (2016) 185–195.
[19] F. Wang, S. He, H. Chen, B. Wang, L. Zheng, M. Wei, D.G. Evans, X. Duan, J. Am. Chem. Soc. 138 (2016) 6298–6305.
[20] J. Xu, X. Su, H. Duan, B. Hou, Q. Lin, X. Liu, X. Pan, G. Pei, H. Geng, Y. Huang, T. Zhang, J. Catal. 333 (2016) 227–237.
[21] M. Gratzel, J. Kiwi, K.R. Thampi, Mixed ruthenium catalyst, Google Patents 1989.
[22] F. Solymosi, A. Erdohelyi, M. Kocsis, J. Chem. Soc. Faraday Trans. Phys. Chem. Condensed Phases 77 (1981) 1003–1012.
[23] P. Panagiotopoulou, D.I. Kondarides, X.E. Verykios, J. Phys. Chem. C 115 (2011) 1220–1230.
[24] B.H. Sakakini, J. Mol. Catal. A: Chem. 127 (1997) 203–209.
[25] J.W.A. Sachtler, J.M. Kool, V. Ponec, J. Catal. 56 (1979) 284–286.
[26] S. Rönsch, J. Schneider, S. Matthischke, M. Schlüter, M. Götz, J. Lefebvre, P. Prabhakaran, S. Bajohr, Fuel 166 (2016) 276–296.
[27] X. Su, J. Xu, B. Liang, H. Duan, B. Hou, Y. Huang, J. Energy Chem. 25 (2016) 553–565.
[28] S. Ma, W. Song, B. Liu, H. Zheng, J. Deng, W. Zhong, J. Liu, X.-Q. Gong, Z. Zhao, Catal. Sci. Technol. 6 (2016) 6128–6136.
[29] P. Panagiotopoulou, D.I. Kondarides, X.E. Verykios, Appl. Catal. A: Gen. 344 (2008) 45–54.
[30] P. Panagiotopoulou, Appl. Catal. A: Gen. 542 (2017) 63–70.
[31] M.S. Duyar, A. Ramachandran, C. Wang, R.J. Farrauto, J. CO2 Util. 12 (2015) 27–33.
[32] G. Garbarino, D. Bellotti, E. Finocchio, L. Magistri, G. Busca, Catal. Today 277 (Part 1) (2016) 21–28.
[33] F. Wang, C. Li, X. Zhang, M. Wei, D.G. Evans, X. Duan, J. Catal. 329 (2015) 177–186.
[34] Z. Kowalczyk, K. Stołecki, W. Raróg-Pilecka, E. Miśkiewicz, E. Wilczkowska, Z. Karpiński, Appl. Catal. A: Gen. 342 (2008) 35–39.
[35] Q. Pan, J. Peng, S. Wang, S. Wang, Catal. Sci. Technol. 4 (2014) 502–509.
[36] D. Wierzbicki, R. Debek, M. Motak, T. Grzybek, M.E. Gálvez, P. Da Costa, Catal. Commun. 83 (2016) 5–8.
[37] G. Zhou, H. Liu, K. Cui, A. Jia, G. Hu, Z. Jiao, Y. Liu, X. Zhang, Appl. Surf. Sci. 383 (2016) 248–252.
[38] M. Agnelli, M. Kolb, C. Mirodatos, J. Catal. 148 (1994) 9–21.
[39] M. Agnelli, H.M. Swaan, C. Marquez-Alvarez, G.A. Martin, C. Mirodatos, J. Catal. 175 (1998) 117–128.
[40] D.C. Upham, A.R. Derk, S. Sharma, H. Metiu, E.W. McFarland, Catal. Sci. Technol. 5 (2015) 1783–1791.
[41] Z.L. Zhang, A. Kladi, X.E. Verykios, J. Catal. 148 (1994) 737–747.
[42] A. Erdöhelyi, M. Pásztor, F. Solymosi, J. Catal. 98 (1986) 166–177.
[43] F. Solymosi, I. Tombácz, J. Koszta, J. Catal. 95 (1985) 578–586.
[44] A.T. Bell, J. Mol. Catal. A: Chem. 100 (1995) 1–11.
[45] F.J. Williams, R.M. Lambert, Catal. Lett. 70 (2000) 9–14.
[46] X. Hu, G. Lu, Green Chem. 11 (2009) 724–732.
[47] T.K. Campbell, J.L. Falconer, Appl. Catal. 50 (1989) 189–197.
[48] M. Guo, G. Lu, RSC Adv. 4 (2014) 58171–58177.
[49] H. Takano, H. Shinomiya, K. Izumiya, N. Kumagai, H. Habazaki, K. Hashimoto, Int. J. Hydrogen Energy 40 (2015) 8347–8355.
[50] W. Ahmad, A. Al-Matar, R. Shawabkeh, A. Rana, J. Environ. Chem. Eng. 4 (2016) 2725–2735.
[51] I. Kalaitzidou, M. Makri, D. Theleritis, A. Katsaounis, C.G. Vayenas, Surf. Sci. 646 (2016) 194–203.
[52] W. An, F. Xu, D. Stacchiola, P. Liu, ChemCatChem 7 (2015) 3865–3872.
[53] M.S. Duyar, S. Wang, M.A. Arellano-Treviño, R.J. Farrauto, J. CO2 Util. 15 (2016) 65–71.
[54] D. Li, N. Ichikuni, S. Shimazu, T. Uematsu, Appl. Catal. A: Gen. 172 (1998) 351–358.
[55] F.M. Hoffmann, M.D. Weisel, Surf. Sci. Lett. 253 (1991) L402–L406.
[56] D. Heyl, U. Rodemerck, U. Bentrup, ACS Catal. 6 (2016) 6275–6284.
[57] C.G. Visconti, M. Martinelli, L. Falbo, A. Infantes-Molina, L. Lietti, P. Forzatti, G. Iaquaniello, E. Palo, B. Picutti, F. Brignoli, Appl. Catal. B: Environ. 200 (2017) 530–542.
[58] R. Satthawong, N. Koizumi, C. Song, P. Prasassarakich, Top. Catal. 57 (2014) 588–594.
[59] H. Kusama, H. Arakawa, Nippon Kagaku Kaishi 2002 (2002) 107–110.
[60] Y. Wang, Y. Zhai, D. Pierre, M. Flytzani-Stephanopoulos, Appl. Catal. B: Environ. 127 (2012) 342–350.
[61] P. Panagiotopoulou, D.I. Kondarides, J. Catal. 267 (2009) 57–66.
[62] Y. Zhai, D. Pierre, R. Si, W. Deng, P. Ferrin, A.U. Nilekar, G. Peng, J.A. Herron, D.C. Bell, H. Saltsburg, M. Mavrikakis, M. Flytzani-Stephanopoulos, Science 329 (2010) 1633–1636.
[63] B. Zugic, D.C. Bell, M. Flytzani-Stephanopoulos, Appl. Catal. B: Environ. 144 (2014) 243–251.
[64] B. Zugic, S. Zhang, D.C. Bell, F. Tao, M. Flytzani-Stephanopoulos, J. Am. Chem. Soc. 136 (2014) 3238–3245.
[65] H. Xie, J. Lu, M. Shekhar, J.W. Elam, W.N. Delgass, F.H. Ribeiro, E. Weitz, K.R. Poeppelmeier, ACS Catal. 3 (2013) 61–73.
[66] H.N. Evin, G. Jacobs, J. Ruiz-Martinez, G.A. Thomas, B.H. Davis, Catal. Lett. 120 (2008) 166–178.
[67] G. Jacobs, B.H. Davis, Int. J. Hydrogen Energy 35 (2010) 3522–3536.
[68] J.H. Pazmiño, M. Shekhar, W. Damion Williams, M. Cem Akatay, J.T. Miller, W. Nicholas Delgass, F.H. Ribeiro, J. Catal. 286 (2012) 279–286.
[69] P. Panagiotopoulou, D.I. Kondarides, J. Catal. 260 (2008) 141–149.
[70] M. Kourtelesis, P. Panagiotopoulou, X.E. Verykios, Catal. Today 258 (2015) 247–255.
[71] A. Swapnesh, V.C. Srivastava, I.D. Mall, Chem. Eng. Technol. 37 (2014) 1765–1777.
[72] P. Kangvansura, L.M. Chew, W. Saengsui, P. Santawaja, Y. Poo-arporn, M. Muhler, H. Schulz, A. Worayingyong, Catal. Today 275 (2016) 59–65.
[73] B. Liang, H. Duan, X. Su, X. Chen, Y. Huang, X. Chen, J.J. Delgado, T. Zhang, Catal. Today 281 (Part 2) (2017) 319–326.
[74] M.L. Ang, U. Oemar, Y. Kathiraser, E.T. Saw, C.H.K. Lew, Y. Du, A. Borgna, S. Kawi, J. Catal. 329 (2015) 130–143.
[75] M. Amoyal, R. Vidruk-Nehemya, M.V. Landau, M. Herskowitz, J. Catal. 348 (2017) 29–39.
[76] D.C. Grenoble, M.M. Estadt, D.F. Ollis, J. Catal. 67 (1981) 90–102.
[77] M. Primet, J. Catal. 88 (1984) 273–282.
[78] R.D. Gonzalez, H. Miura, J. Catal. 77 (1982) 338–347.
[79] M.M. McClory, R.D. Gonzalez, J. Catal. 89 (1984) 392–403.
[80] T. Mori, A. Miyamoto, N. Takahashi, H. Niizuma, t. Hattori, Y. Murakami, J. Catal. 102 (1986) 199–206.
[81] C.G. Vayenas, S. Brosda, C. Pliangos, J. Catal. 203 (2001) 329–350.
[82] D. Theleritis, M. Makri, S. Souentie, A. Caravaca, A. Katsaounis, C.G. Vayenas, ChemElectroChem 1 (2014) 254–262.
[83] J. Benziger, R.J. Madix, Surf. Sci. 94 (1980) 119–153.
[84] M.P. Kiskinova, Surf. Sci. 111 (1981) 584–594.
[85] D. Tománek, K.H. Bennemann, Surf. Sci. 127 (1983) L111–L117.
[86] D.A. Wesner, G. Linden, H.P. Bonzel, Appl. Surf. Sci. 26 (1986) 335–356.
[87] I.-G. Bajusz, D.J. Kwik, J.G. Goodwin, Catal. Lett. 48 (1997) 151–157.